Nonuniform structural degradation in porous organosilicate films exposed to plasma, etching, and ashing as characterized by x-ray porosimetry

Hae-Jeong Lee, Christopher L. Soles,[a] Eric K. Lin, and Wen-li Wu
Polymers Division, National Institute of Standards and Technology, Gaithersburg, Maryland 20899, USA

Youfan Liu
Intel Corporation, Chandler, Arizona 85266, USA

(Received 9 August 2007; accepted 28 September 2007; published online 25 October 2007)

X-ray porosimetry is used to characterize the porosity, the average film density, and the density of the wall material between the pores in ultralow-*k* films as a function of film thickness. These measurements are performed on films that have been plasma treated as well as plasma etched and an ashed to evaluate how these integration processes affect the pore characteristics of the interlayer dielectric. The damage, a decrease of porosity and an increase in the wall density, is strongly localized to the exposed surface of the film. The plasma etching and ashing tend to induce more surface damage than the plasma alone. © *2007 American Institute of Physics*.
[DOI: 10.1063/1.2800376]

It is well-known that porous low dielectric constant (low-*k*) materials are more vulnerable to plasma processing in comparison to their nonporous analogs because pores enhance chemical reactions with the reactive species in the plasma.[1] There have been tremendous efforts to develop and optimize the processing parameters to minimizing the plasma-induced damage of low-*k* films through systematically establishing process-structure relationships.[1,2] However, the nondestructive determination of porous structure through the thickness of a film is an important measurement challenge for developing effective integration schemes for interconnects. Currently, there are only a few techniques available to profile the plasma-induced damage in porous thin films, including positron annihilation lifetime spectroscopy (PALS) and variable angle spectroscopic ellipsometry (VASE).[3–5] With PALS, one can vary the implantation energy of the positron beam to control the effective localization depth of the positron and therefore to extract the pore size information as a function of depth.[4] In VASE, the measured optical parameters, Ψ and Δ as a function of wavelength and/or spectroscopic angle, are compared with the calculated values based on a model with a given variation in the porosity as a function of depth to see if the proposed model is consistent with the experimental data.[5] However, there are model-dependent limitations with each technique and additional challenges to profile porosity in a film with nanometer-type resolution.

The aim of this letter is to present an x-ray porosimetry (XRP) based methodology to determine the porosity and density depth profiles in porous low-*k* dielectric thin films that have vertically nonuniform profiles as a result of plasma-induced damage. This type of metrology is critical to understand the effects of the integration processes on the porous thin films and to further optimize the processing conditions. As-vitrified porous films with an ultralow-*k* of approximately 2.2 were post-treated in two different conditions. One of the films was exposed to N_2O plasma surface treatment, while the other was first dry etched and then exposed to N_2/H_2 containing plasma to represent the surface ashing processes. The two samples are denoted as spin-on-glass (SOG)/plasma and SOG/etching/ashing, respectively.

XRP is a nondestructive, on-wafer characterization methodology utilizing specular x-ray reflectivity (SXR) and has been used to determine the pore structures of porous low-*k* thin films.[6,7] Here, SXR measurements were performed under vacuum, a saturated toluene atmosphere, and 100% relative humidity to determine the porosity and hydrophilicity of the films. These saturated environments were created by breaking the vacuum and placing containers of either liquid toluene or water inside the SXR chamber. The detailed SXR measurements and data analysis were performed in a manner reported elsewhere.[8]

Figure 1 shows experimental SXR data and the fits to extract the density profiles for the SOG/plasma and SOG/

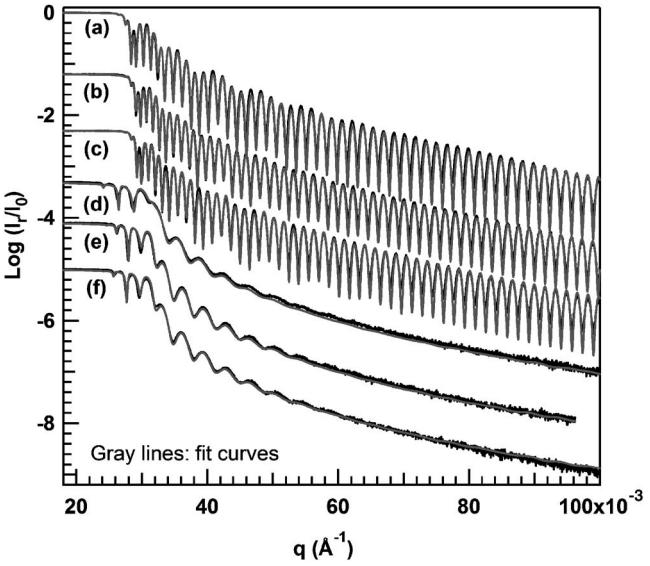

FIG. 1. The experimental SXR data (black lines) and the best fits (gray lines). I_r and I_0 indicate the reflected and incident beam intensities. Curves (a)–(c) correspond to the plasma treated surfaces, while (d)–(f) correspond to the films exposed to the etching/ashing process.

[a]Author to whom correspondence should be addressed. Electronic mail: csoles@nist.gov.

etching/ashing samples under vacuum [curves (a) and (d)] in the saturated toluene [curves (b) and (e)] and in the 100% relative humidity environment [curves (c) and (f)]. There are two critical angles at low q displaying sharp drops in intensity, beyond which periodic interference fringes in the reflectivity are observed. These critical angles are associated with the average electron density of the layers through the equation, $q_c^2 = 16\pi\rho_e r_e$, where ρ_e is the electron density and r_e is the classical electron radius. The first critical angle in the SXR data notably shifts to higher q values in the presence of probe solvent due to the capillary condensation of the solvent inside the pores. This is a result of the large increase in the density of the porous film. Qualitatively, a multilayer structure is anticipated from the beating of multiple periodicities in the low q interference fringes of samples treated with the plasma. The highest frequency oscillations beyond the critical angle are classic, the well-defined Kiessig fringes typical of a film of finite thickness, while low frequency oscillation between the critical angles of the ultralow-k materials and the underlying silicon substrate confirm the existence of sublayer at the surface or interface of low-k film. However, this low frequency oscillation is not obvious for the samples condensed with toluene, which can be anticipated from a smaller contrast of electron density between wall material and filled pores with toluene solvent in comparison to the large contrast between wall material and empty pores (i.e., vacuum).

The etching/ashing process induces a dramatic decreases in frequency of the Kiessig interference fringes over the full q range, indicating decreases in total film thickness. The film thickness t is inversely proportional to the periodicity of the oscillations Δq ($t \sim 2\pi/\Delta q$ well beyond the critical angles).[8,9] The other noticeable change in the reflectivity upon etching/ashing is a reduction in the amplitude of the Kiessig fringes that increases with q, indicative of an increase in the film roughness. The detailed structural characteristics of the porous films can be quantified by fitting the SXR data to model density profiles based on the algorithm of Parratt.[10] The number of layers, their thickness, density, and interfacial roughness of the model profiles are reiteratively adjusted until the calculated reflectivity best fits the experimental data. The films here required either three or two layers to fit the data, depending on the type of postprocessing. To discretize the density profile into two or three well defined layers is, of course, a simplification; the real profiles are probably smoothed. However, the model is sufficiently accurate to parametrize the experimental data and a reasonable approximation. These fitted density profiles are graphically shown in Fig. 2 as a function of film depth, while Table I summarizes the numerical values for the thickness and scattering length density (SLD or q_c^2) of each layer. In the SLD density profiles, notice roughness term has the same effect as increasing the breadth of the interface.

All of the films show that the processing, either the plasma or the etching and ashing, increases the density at the free surface of the films. A dense skin layer is not observed for the as-vitrified SOG films. For the SOG/plasma samples, the SLD of low-k film increases through three layers, starting with 4.32×10^{-4} Å^{-2} near the Si substrate and increases to 7.32×10^{-4} Å^{-2} at the free surface, approximately a 70% increase in density.[11] This observation is consistent with plasma densifying the porous material. In the presence of the toluene probe solvent, the density profile of the SOG/plasma film shows qualitatively similar three layer variations in density. However, the density of each layer increases differently with respect to their vacuum values. These data indicate that the porosities of the three layers are very different.

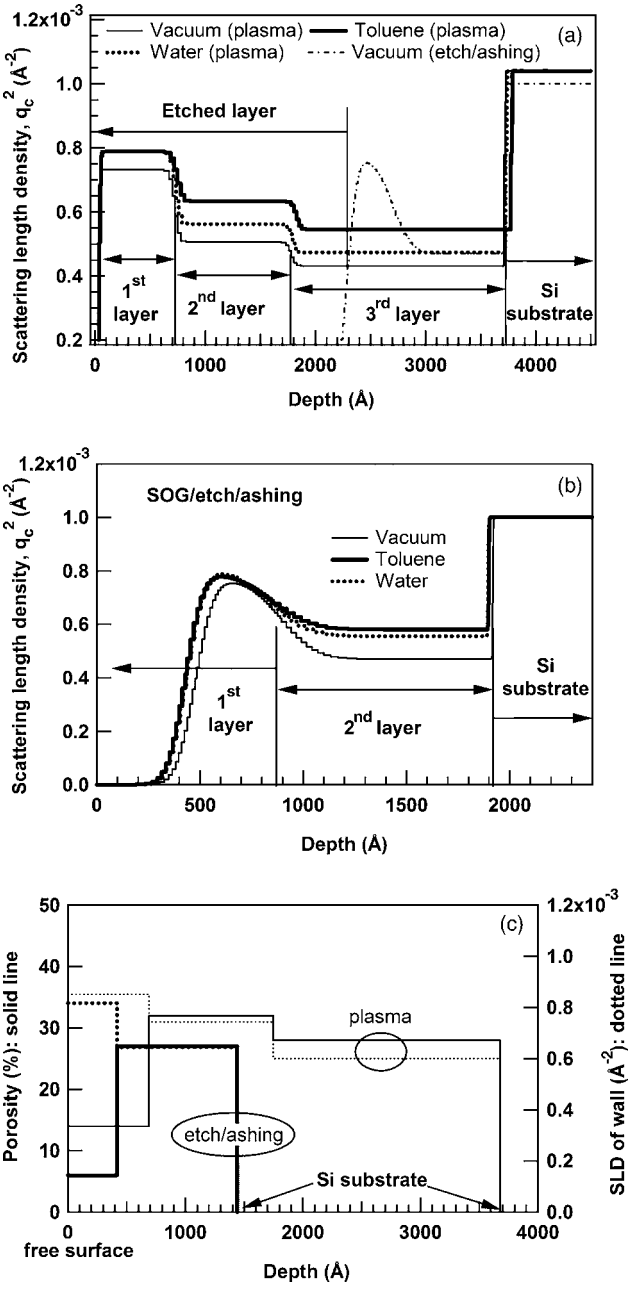

FIG. 2. The density profiles obtained from the fits to the experimental data in Fig. 1 are shown in terms of the SLD as a function of depth through the film. Parts (a) and (b) correspond to the films processed by plasma and etching/ashing treatments, respectively. The variations in porosity and wall density of the different layers are shown as a function of depth into the film in part (c).

The porosity of each layer can be calculated from solvent uptake of that layer (in the unit of g/cm^3) divided by the mass density of the solvent (here, we assume $\rho_{\text{solvent}} = 0.865$ g/cm^3 for the toluene and 1.00 g/cm^3 for water, respectively). The solvent uptake is determined by subtracting the average electron density determined under vacuum ($\rho_{e,\text{vacuum}}$) from that determined in saturated atmosphere ($\rho_{e,\text{solvent}}$) for each layer, as shown in Eq. (1).

TABLE I. The average scattering length density (SLD) and thickness (t) of the SOG/plasma and SOG/etching/ashing films. The relative standard uncertainties of the SLD, film thickness, and porosity are $\pm 0.01 \times 10^{-4}$ Å^{-2}, ±10 Å, and ±1%, respectively.

		Average density, SLD/10^{-4} (Å^{-2}) and thickness t (Å)								
		Vacuum		Toluene		Water		Porosity (%)	Wall density, SLD/10^{-4} (Å^{-2})	Fraction of pores filled with water (%)
Samples	Layer	SLD	t	SLD	t	SLD	t			
SOG/plasma	First	7.32	691	7.88	708	7.89	696	14	8.51	86
	Second	5.05	1056	6.33	1080	5.63	1056	32	7.43	38
	Third	4.32	1931	5.45	1945	4.74	1933	28	6.00	32
SOG/etching/ashing	First	7.68	418	7.92	424	8.05	412	6	8.17	100
	Second	4.70	1024	5.80	1045	5.55	1050	27	6.44	65

$$P = \frac{\text{solvent uptake}}{\rho_{\text{solvent}}} = \frac{(\rho_{e,\text{solvent}} - \rho_{e,\text{vacuum}})MW_{\text{solvent}}}{n_{e,\text{solvent}} N_A \rho_{\text{solvent}}}, \quad (1)$$

with $\rho_e = \pi\theta_c^2/\lambda^2 r_e$ and $\theta_c^2 = [\arcsin(\lambda\sqrt{Q_c^2}/4\pi)]^2$, where MW_{solvent}, $n_{e,\text{solvent}}$, and N_A are molecular mass of solvent, total number of electrons in a solvent molecule, and Avogadro's numbers, respectively. This way, the porosity is defined as the volume of the pores filled by the solvent relative to the volume of the film (defined by the thickness). This definition assumes that all the pores can be accessed by the toluene probe molecules. This is a reasonable assumption given that a small but perceivable swelling in the film thickness [approximately (0.2–1.9%) by height] occurs in the toluene environment. Toluene likes the material sufficiently to penetrate the film but excessive swelling is prohibited by the highly cross-linked nature of the film.

For the SOG/plasma films, the free surface shows a dramatic decrease in porosity and an increase in wall density, approximately 50% and 42%, respectively, in comparison to the third layer nearest the Si substrate. This result means that the plasma process not only induces a collapse of pores but also densifies the wall material between the pores. This increase in the wall density is probably due to a depletion of carbon in the material.[12] Interestingly, the porosity of the second layer remains unchanged (if anything slightly higher), while wall density of the second layer increases approximately 24% relative to that of the third layer. Therefore, the most significant factor affecting the increased film density during the plasma treatment should be the densification of wall material; the pore collapse appears to be a secondary effect here. Carbon depletion is evidenced by the fraction of pores filled with water Φ_w which is determined from the ratio of porosity under 100% of relative humidity to porosity in saturated toluene ($P_{\text{water}}/P_{\text{toluene}}$). The Φ_w values for each layer are summarized in Table I. When the carbon content decreases, the pore surface becomes more hydrophilic and water has a stronger propensity to wet the pores. This change in surface chemistry allows more pores to be filled by water. Therefore, the degree of carbon depletion can be qualitatively inferred from Φ_w. The layer closest to the damaged (free) surface shows larger Φ_w values, confirming hydrophilic surface.

In the case of etching/ashing sample, a simple two layer model is used to fit the experimental data. As displayed in Table I, the entire film is affected and SLD of the entire thickness is increased by the etching/ashing process. The damage at the free surface exposed to the etching/ashing environment is more severe, resulting in a 78% increase over the initial SLD, while SLD of the second layer increases by only 9%. Here, initial SLD of etching/ashing sample is assumed to be the same as the third layer of the plasma treated sample. Furthermore, the etching/ashing process dramatically decreases the film thickness from 3678 to 1442 Å, almost a 60% change in thickness. When the porosities of these layers are determined, we see that etching/ashing is more damaging compared to the plasma treatment, reducing the porosity all the way down to 6%. Moreover, both layers show a large Φ_w indicating a hydrophilic characteristic in comparison to original film. This induced hydrophilicity is potentially problematic, as it could degrade performance of an interconnect device. As shown in Fig. 2(c), porosity and wall material density profiles are plotted as a function of distance from Si substrate to visualize damage induced by the plasma and etching/ashing processes.

In conclusion XRP has the ability to characterize the details of the porous structure with high sensitivity and to correlate changes with the processing conditions, allowing optimization of the integration processes. Here we have shown how it can be used to quantify the densification of an SOG film upon plasma and etching/ashing exposure.

The authors would like to acknowledge the NIST Office of Microelectronics Programs for their financial support of this research.

[1] K. Yonekura, S. Sakamori, K. Goto, M. Matsuura, N. Fujiwara, and M. Yoneda, J. Vac. Sci. Technol. B **22**, 548 (2004).
[2] A. Sankaran and M. Kushner, Appl. Phys. Lett. **82**, 1824 (2003).
[3] C. L. Wang, M. H. Weber, and K. G. Lynn, J. Appl. Phys. **99**, 113514 (2006).
[4] J. N. Sun, D. W. Gidley, Y. Hu, W. E. Frieze, and E. T. Ryan, Appl. Phys. Lett. **81**, 1447 (2002).
[5] M. T. Othman, J. A. Lubguban, A. A. Lubguban, S. Gangopadhyay, R. D. Miller, W. Volksen, and H. C. Kim, J. Appl. Phys. **99**, 083503 (2006).
[6] H. J. Lee, E. K. Lin, B. J. Bauer, W. L. Wu, B. K. Hwang, and W. D. Gray, Appl. Phys. Lett. **82**, 1084 (2003).
[7] H. J. Lee, C. L. Soles, D. W. Liu, B. J. Bauer, E. K. Lin, W. L. Wu, and A. Grill, J. Appl. Phys. **95**, 2355 (2004).
[8] W. L. Wu, W. E. Wallace, E. K. Lin, G. W. Lynn, C. J. Glinka, E. T. Ryan, H. M. Ho, J. Appl. Phys. **87**, 1193 (2000).
[9] C. E. Bouldin, W. E. Wallace, G. W. Lynn, S. C. Roth, and W. L. Wu, J. Appl. Phys. **88**, 961 (2000).
[10] L. G. Parratt, Phys. Rev. **95**, 359 (1954).
[11] The data throughout the manuscript and in figures and table are presented along with the standard uncertainty (±) involved in the measurement based on one standard deviation.
[12] X. Hua, M. Kuo, G. S. Oehrlein, P. Lazzeri, E. Lacob, M. Anderle, C. K. Inoki, T. S. Kuan, P. Jiang, and W. L. Wu, J. Vac. Sci. Technol. B **24**, 1238 (2006).